Satellite interferometric data for seismic damage assessment

Available online at www.sciencedirect.com

ScienceDirect

Procedia Structural Integrity 44 (2023) 1570–1577

Structural Integrity Procedia

www.elsevier.com/locate/procedia

XIX ANIDIS Conference, Seismic Engineering in Italy

Satellite interferometric data for seismic damage assessment

Pier Francesco Giordano[a,*], Gaetano Miraglia[b], Erica Lenticchia[b], Rosario Ceravolo[b], Maria Pina Limongelli[a]

[a]*Department of Architecture, Built Environment and Construction Engineering (DABC), Politecnico di Milano, Piazza Leonardo da Vinci, 32, 20133 Milano, Italy*

[b]*Department of Structural, Geotechnical and Building Engineering (DISEG), Politecnico di Torino, Corso Duca degli Abruzzi, 24 10129 Torino, Italy*

Abstract

Radar satellites allow the collection of data on large areas without direct access to structures. Thereby, they appear very attractive for Structural Health Monitoring (SHM) purposes. Data collected by satellites can be processed to obtain temporal histories of displacements through which the health state of a monitored system can be potentially identified. However, anomalies in the time histories of displacements are not necessarily due to damage. Environmental phenomena, such as variations in atmospheric temperature, and rain, can modify the behavior of structures without compromising their safety. The impact of these phenomena on the structural response can hinder the identification of anomalies or lead to false alarms if such alterations are misinterpreted as damage. Furthermore, if the monitored system is a historical structure, uncertainties on the structural behavior are inevitably increased during aging. The purpose of this article is to discuss the possibility of identifying damage due to seismic actions considering the impact of variations of environmental factors on the time histories of the displacements retrieved by satellite data. The structural health condition of a historical structure located in the city of Rome (Italy) hit by the October 2016 Central Italy earthquakes is investigated based on interferometric satellite data. The satellite data are acquired by COSMO-SkyMed (CSM) of the Italian Space Agency between 2010 and 2019 and are processed by CNR IREA.

Peer-review under responsibility of the scientific committee of the XIX ANIDIS Conference, Seismic Engineering in Italy.

Keywords: Structural Health Monitoring, Remote sensing, Satellite data, DInSAR, Historical buildings, Seismic Damage.

* Corresponding author.
E-mail address: pierfrancesco.giordano@polimi.it

Peer-review under responsibility of the scientific committee of the XIX ANIDIS Conference, Seismic Engineering in Italy.
10.1016/j.prostr.2023.01.201

1. Introduction

Earthquakes affect large areas and can cause vast damage. In turn, the management of the built environment in the aftermath of a seismic event is a critical issue for authorities that have to prioritize inspections and assess the conditions of a large number of structures and infrastructures. Generally, the presence and the extent of damage are evaluated through visual inspections performed by expert technicians who assign a score to each structure relating to its safety and usability. Nevertheless, performing visual inspections generally requires a significant amount of time and resources. In this context, automatic Structural Health Monitoring (SHM) systems can provide real-time information on the state of structures thus supporting decision-makers (Giordano et al., 2022; Rainieri et al., 2020; Zhang et al., 2023). The main drawback of traditional SHM systems relates to the costs associated with deploying sensors on structures. Furthermore, the physical components of SHM systems degrade in time and require continuous maintenance. Thus, it is not generally feasible to instrument all the buildings in a city or the bridges in a transportation network. In this respect, remote sensing techniques can provide an appealing alternative to traditional SHM systems.

In the last decades, data acquired from satellites equipped with Synthetic Aperture Radar (SAR) have been used to monitor deformations of the Earth's surface. More recently, thanks to the increasing spatial resolution, the monitoring of civil structures is an object of study (Delo et al., 2022; Farneti et al., 2022; Macchiarulo et al., 2022). SAR satellite monitoring techniques are based on the study of the phase difference between pairs of SAR images acquired over the same area in different moments to follow the deformation of the Earth's surface in time. The results of these techniques are Persistent Scatter (PS) associated with spatial coordinates and a Line-of-Sight (LOS) displacement time series. The main advantages of SAR satellite monitoring relate to the possibility of monitoring very large areas and going back in time without the need of installing sensors on the structures.

The goal of this paper is to investigate the use of SAR satellite data to identify seismic damage on structures following a seismic event. The case study examined is the Basilica of Saint Paul Outside the Walls, in Rome, Italy, that has been slightly damaged on October 30 by a 6.5 magnitude earthquake with an epicenter located in the proximity of Norcia, in Central Italy. According to the principle of minimum intervention (ICOMOS/ISCARSAH, 2005), SAR satellite monitoring appears particularly indicated for cultural heritage structures.

SAR satellite data used in this study were made available by CNR IREA in the context of the ReLUIS project "Structural Health Monitoring and satellite data". Displacements are computed by using SAR data from COSMO-SkyMed (CSK) of the Italian Space Agency. Satellite data cover a long period (July 2011 – March 2019) in StripMAP HIMAGE mode (spatial resolution 3 m). The dataset has been processed using a DInSAR (Differential Interferometric Synthetic Aperture Radar) technique based on the "Parallel SBAS Interferometry Chain" (Berardino et al., 2002).

LOS displacement data are first processed using a technique presented in (Giordano et al., 2022) based on the study of the mean displacement of influence areas of the investigated structure and also using spectral entropy measures. If on one hand, the mean displacement can provide a straightforward interpretation of the building behavior over the years, thus allowing direct control of what is happening to a structure, on the other hand, entropy can add useful information on the evolution of the power spectral distribution in time (Miraglia et al., 2023), and thus deepening the evaluation of the building behavior at several frequency bandwidths. Because the entropy of data gathered by a system decreases in presence of input of energy, or simply changes in case of permanent structural modifications, entropy is particularly important for two reasons (Ceravolo et al., 2021; West et al., 2019): (i) to detect variations (in terms of amplitude and frequency) of the input sources; (ii) detect changes in the structural properties of a system (which in turn are reflected in a variation of the amplitude and frequency response of the structure, if supposed subjected to a time-invariant input source).

The paper is organized as follows: Section 2 presents the case study; Section 3 describes the dataset used in the analyses, which is composed by DInSAR displacement gathered by satellite; Section 4 reports the influence area method and the processing outputs; while Section 5 contains the spectral entropy analysis, aimed to cross-check results of the former analysis; finally, the results and conclusions are drawn in Section 6.

2. Case study: Basilica of Saint Paul Outside the Walls

The basilica rises above the Roman necropolis where the apostle Paul, from whom it takes its name, was buried. During its life, the basilica has undergone continuous transformations. In the year 324, the emperor Constantine

erected the first building. In the following years, it was enlarged by the architect Ciriade, who designed a basilica consisting of five naves and a four-sided portico. The works of the new basilica ended in the year 395. At the end of the 9th century, Pope John VIII added walls and towers to protect the structure from the Lombards and Saracens. In the 11th century, a bell tower was erected next to the facade. Over the centuries, the basilica was continually restored and embellished but its structure remained the original one. On the night of July 15, 1823, a disastrous fire almost destroyed the original basilica and the works of art it contained. The reconstruction of the basilica began in September 1826 under the guidance of Pasquale Belli who was working on a project by Giuseppe Valadier. Starting from 1833, the reconstruction works were entrusted to Luigi Poletti who determined the current Paleochristian aspect of the basilica. In 1928, the vast external quadriporticus was built by Guglielmo Calderini. Since 1980, the Basilica is a UNESCO World Heritage Site.

On October 30, 2016, the Basilica was hit by one of the main shocks of the 2016–2017 Central Italy earthquake sequences. Thus, the Basilica was closed to the public and inspected by technicians due to the occurrence of minor damage such as the opening of cracks and detachment of cornices. In particular, the presence of cracks on the front side of the quadriporticus was reported, see online photographs (repubblica.it, 2016).

Figure 1. Façade of the Basilica.

3. DInSAR displacement data

CNR IREA has processed CSK data acquired over the period between 2010 and 2019 and covering the area of Rome using the DInSAR technique. The results of the analysis consist of a list of PSs to which several data are associated, such as identification numbers, coordinates, mean velocity, coherence, and LOS displacement over time. In this study, only data from the Descending orbit are employed. A Geographic Information System (GIS) software is used to display the PSs on the Earth's surface and identify those belonging to the structure under investigation. Figure 3 shows the PSs located in the proximity of the Basilica of Saint Paul and those located on the quadriporticus. The PS color indicates the mean velocity along the LOS over the observation period. Most of the PSs present negative velocities, indicating that they are moving away from the satellite.

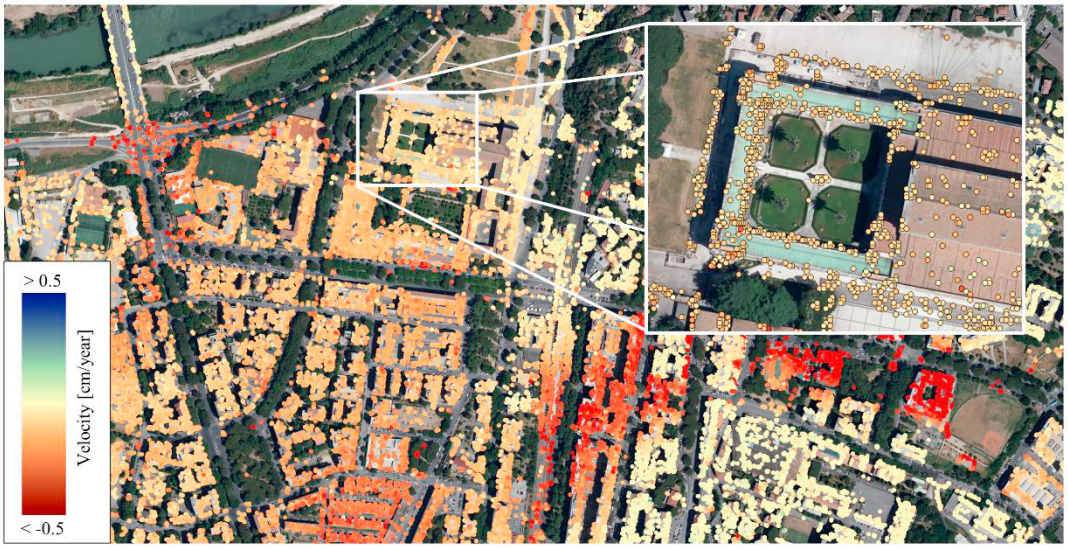

Figure 2. PSs in the proximity of the Basilica of Saint Paul and zoom on the quadriporticus. The PS color relates to the mean velocity along the LOS over the observation period.

4. Analysis of reference areas

In this study, the analysis of the effects of the October 30 seismic event through satellite data is limited to the quadriporticus. First, the analysis focuses on the main side of the structure, where most of the cracks have been visually identified. After that, the analysis is extended to the entire quadriporticus to detect modifications of the global structural behavior. Due to the difficulty of locating in space the PSs belonging to the colonnade, only the PSs on the roof are accounted for in the analysis.

In this section, the analysis of the DInSAR satellite data has been carried out according to (Giordano et al., 2022), and implies the following steps:

- Identification of "influence areas". Four influence areas are identified on the front side of the quadriporticus, see Figure 3(a): two external zones (Areas 1 and 4) which correspond to the corners of the quadriporticus, characterized by large columns, and the two central zones (Areas 2 and 3).
- PS filtering. PSs with anomalous behavior are excluded from the analysis. In this application, only PSs whose average speed is in the range $\pm 2\sigma$ (σ=standard deviation of the average speed within each area) are considered.
- Calculation of mean displacements. Determination of the time history of the mean displacement of the PSs in each influence area.
- Normalization. The displacement time histories of the PSs are relative to different reference (initial) displacements. Therefore, in each influence area, the mean displacement computed in the first two years of observations is subtracted from the entire displacement time series. The underlying assumption behind this step is that damage has not occurred during the initial observation period.

The (normalized) mean displacement of a given influence area is referred to as the "Representative Displacement" (RD) of that area. The estimated RD time histories are shown in Figure 3(b). The time histories do not show a clear seasonal trend. It can be observed that the four RDs have similar behavior in the first years of observation. Instead, starting from the year 2015, two phenomena start occurring. First, in general, the velocity of the RDs (computed over a one-year time window) became noticeably negative. Secondly, the displacements of the external corners (Areas 1 and 4) start differing from those of the central portions of the quadriporticus (i.e., Areas 2 and 3). In turn, Areas 2 and 3 present almost the same trend. Regarding the effects of the earthquake, clear anomalies in the structural behavior following the seismic event cannot be detected.

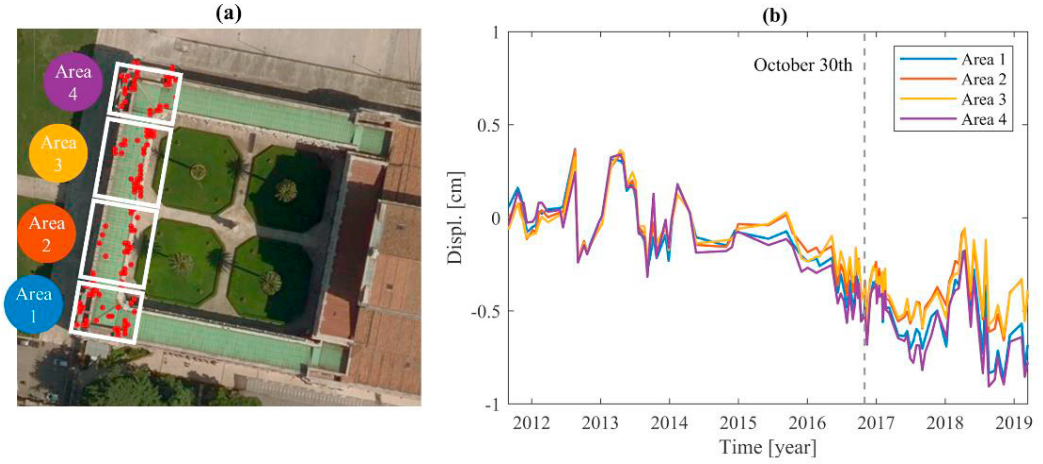

Figure 3. (a) Definition of influence areas – front side of the quadriporticus; (b) RD time histories – front side of the quadriporticus.

The analysis is then extended to the entire quadriporticus. Three influence areas are identified on the quadriporticus, corresponding to the three sides of the structure, see Figure 4(a). In particular, the new Area 2 consists of the union of Areas 2 and 3 in Figure 3(b). The corners of the quadriporticus are not considered in the analysis since - as highlighted above - they present higher displacements. In addition, a fourth RD is computed considering the PSs located on the soil surrounding the monumental complex, highlighted in yellow in Figure 4(a). The RDs are computed following the procedure presented previously. The time histories of the RDs are shown in Figure 4(b). The three influence areas present very similar displacements.

Figure 4(c) displays the time histories of the relative displacements between the RD associated with the soil and the RDs associated with the quadriporticus. The time histories of the relative displacements present a clear seasonal trend, with maximum and minimum displacements respectively in summer and winter.

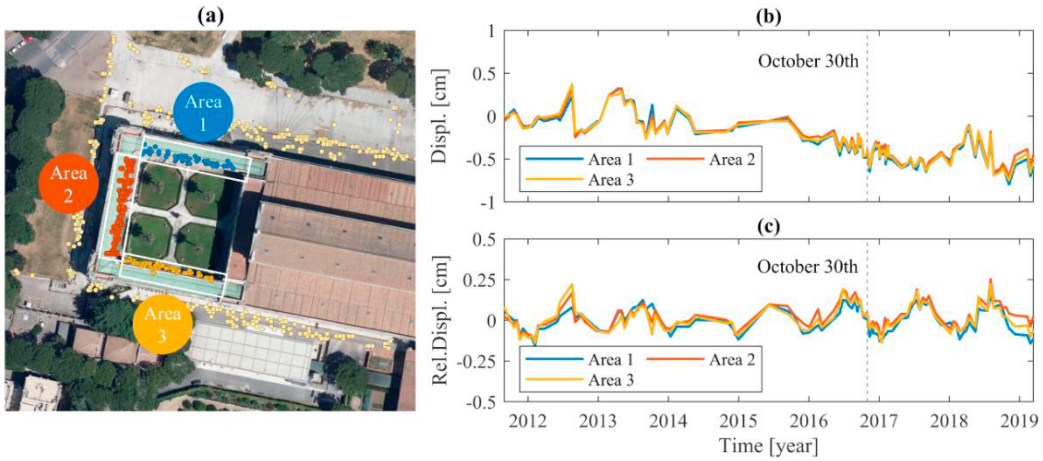

Figure 4. (a) Definition of influence areas – entire quadriporticus; (b) RD time histories – entire quadriporticus; (c) Relative displacements.

After removing the influence of the soil, two additional analyses are carried out: first, a quantitative relationship between the displacements and the temperature is established; after that, the occurrence of modification in the structural behavior is investigated.

To study the relationship between relative displacements and temperature, linear regression lines and associated coefficients of determination R^2 are determined. The temperature data have been recorded by the weather station

"ROMA Lanciani" on the same days when the satellite data were acquired (Regione Lazio, 2020). Mean daily temperature data are used. The results in Figure 5(a) demonstrate the strong correlation between the two quantities. Specifically, the coefficients of determination associated with Areas 1, 2, and 3 are 0.82, 0.71, and 0.78, respectively. Thus, it can be concluded that a linear relationship between relative displacements and environmental temperature exists.

A linear regression model between relative displacements and temperature is established considering the first two years of observations, in which the structure is assumed to be healthy. This linear model is used to predict the three RDs both in the training period and in the following years. The residuals, computed as the difference between the real and the simulated displacements are shown in Figure 5(b). As for Areas 1 and 3, after the training period, the distribution of the residuals does not change significantly in time. Some outliers can be observed in the year 2015. After the year 2015, the magnitude of the residuals in Area 2 increases. The analysis of the residuals does not highlight anomalies following the seismic event of October 30th, 2016.

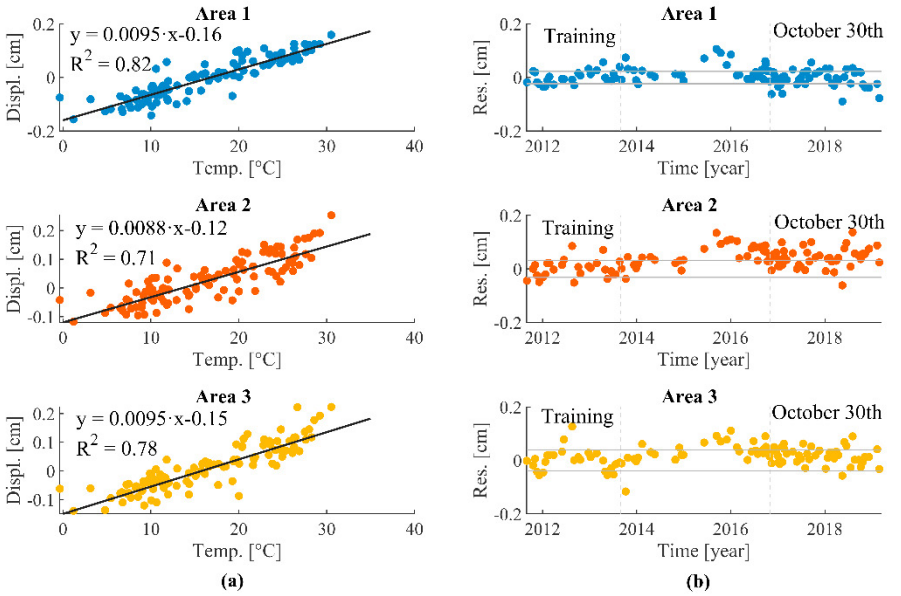

Figure 5. (a) Linear regression lines and (b) residuals between modelled and real displacements.

5. Entropy analysis

Provided a set of data points of a structural system for which the LOS displacements are available, the energy of the signals $E(t)$ in time t, and the Shannon Spectral Entropy $S(t)$ in t can be evaluated. These variables are then correlated together using a time-varying Probability Density Function (pdf) of the Shannon Spectral Entropy, as a function of the signal energy:

$$pdf\big(S(E(t))\big) = \frac{1}{\sigma\big(S(E(t))\big)\sqrt{2\pi}} e^{\left(-\frac{1}{2}\left(\frac{S(E(t))-\mu\left(S(E(t))\right)}{\sigma\left(S(E(t))\right)}\right)^2\right)} \quad (1)$$

$$\mu\big(S(E(t))\big) = e^{p_1 ln^2(E(t))+p_2 ln(E(t))+p_3} \quad (2)$$

$$\sigma\big(S(E(t))\big) = e^{p_4 erf(ln(E(t))-p_5)+p_6} \quad (3)$$

In Eq. (2) and Eq. (3), $\mu\big(S(E(t))\big)$ is the mean value of the entropy, while $\sigma\big(S(E(t))\big)$ represents its time-varying standard deviation, evaluated in each point with energy $E(t)$. Instead, p_i, with i=1,2,3,4,5,6, are model regression

parameters. Defining the "Average of the mean entropy" as the average value of $\mu(S(E(t)))$ inside each Area of the structural system (in this case Area 1, Area 2, and Area 3) it is possible to check its time behavior and study the divergence of the behavior between the areas, to assess if any anomaly is present and in what instant it appeared. Because data are always affected by Environmental and Operational Variations (EOVs), the Average of the mean entropy in each area has been evaluated with different filtering strategy of the raw LOS displacements. The filtering strategy of the data follows the conclusion of a previous work (Miraglia et al., 2023), in which 3 main frequency bandwidths have been defined: multi-year phenomena (<20 [nHz], i.e., > ~19 months), annual phenomena (>20 [nHz], i.e., < ~19 months), and sub-annual phenomena (>50 [nHz], i.e., < ~8 months).
Figure 6 reports the conclusion of the analysis. From the figure it is possible to observe that for any case of analysis, the Average of the mean entropy does not differ between the different areas, suggesting the difficulty of identifying the damage due to the earthquake that raised in Area 2 with this kind of data.

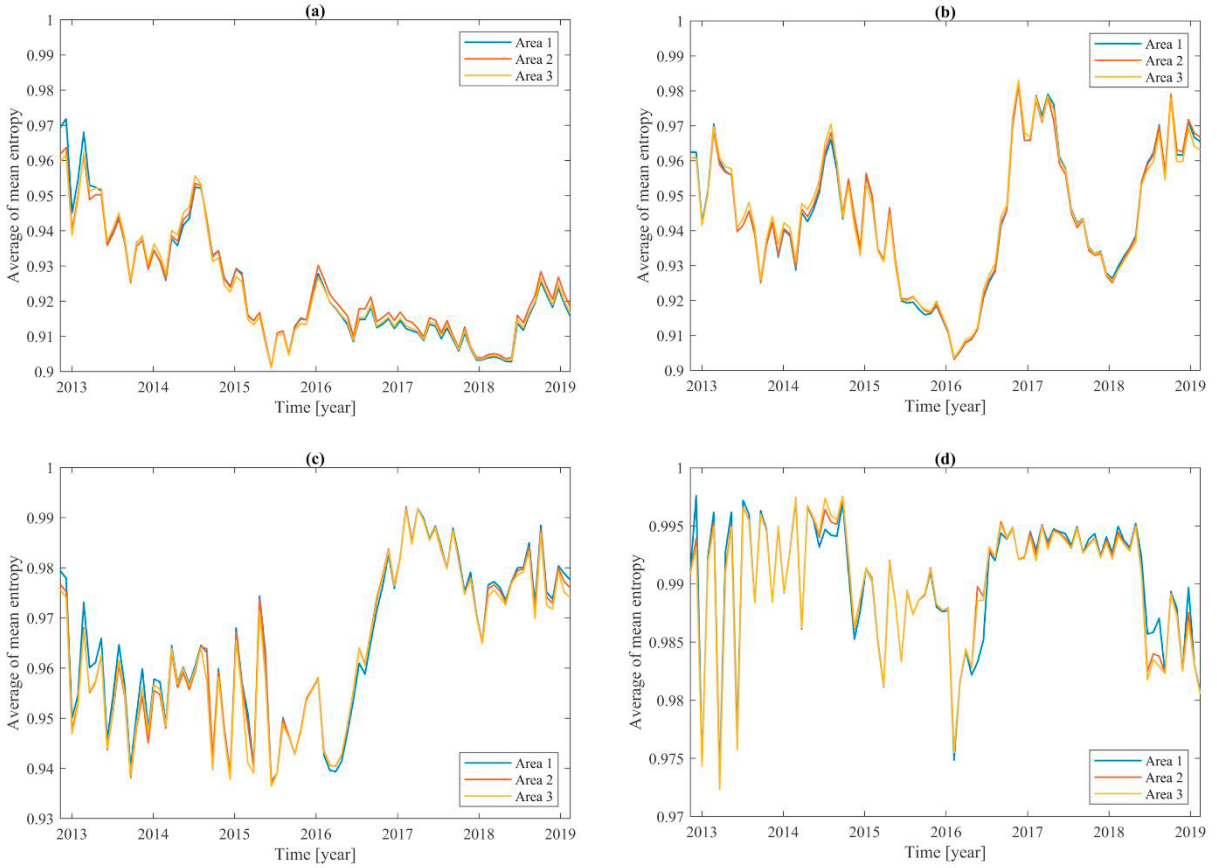

Figure 6. Average value of mean entropy as a function of time. (a) Trends effects (0 [nHz]); (b) Low frequency phenomena effects (<20 [nHz]); (c) Annual phenomena effects (20-50 [nHz]); (d) Sub-annual phenomena effects (>50 [nHz]).

6. Conclusion

This paper discusses the use of SAR satellite data to assess the occurrence of slight seismic damage in buildings in the aftermath of an earthquake. A real case study is investigated, namely the Basilica of Saint Paul Outside the Walls, in Rome, Italy, which was slightly damaged by a seismic event in 2016. SAR satellite data (from CSK) were processed by CNR IREA through the DInSAR technique. Two techniques are used to process LOS displacements, namely the study of the mean displacement of selected influence areas and entropy analysis. The analysis with influence areas

highlights the strong influence of external phenomena on the structural displacements, namely environmental temperature and soil movements, but does not provide any indication of damage following the seismic event. As regards the entropy analysis, it is possible to conclude that the variation of the average of the mean entropy for any sub bandwidth of analysis does not suggest a clear picture of the well-being of the structure, not highlighting differences in the behavior of the 3 blocks, even if one of these (Area 2) suffered visible damage following a seismic event. Small damages seem difficult to detect for observation frequencies in the order of nanohertz, in accordance with the axioms of monitoring.

The results of the study show as the detection and localization of relatively small damages from satellite is still challenging and further effort need to be allocated in understanding the effects of EOVs and/or processing artefacts in the interferometric measures if these want to be used for civil SHM.

Acknowledgments

CNR-IREA is gratefully acknowledged for processing and providing DInSAR-derived data. This study was partially funded by the Italian Civil Protection Department within the WP6 “Structural Health Monitoring and Satellite Data” 2019-21 ReLUIS Project.

References

Berardino, P., Fornaro, G., Lanari, R., & Sansosti, E. (2002). A new algorithm for surface deformation monitoring based on small baseline differential SAR interferograms. *IEEE Transactions on Geoscience and Remote Sensing*, *40*(11), 2375–2383. https://doi.org/10.1109/TGRS.2002.803792

Ceravolo, R., Civera, M., Lenticchia, E., Miraglia, G., & Surace, C. (2021). Detection and Localization of Multiple Damages through Entropy in Information Theory. *Applied Sciences*, *11*(13), 5773. https://doi.org/10.3390/app11135773

Delo, G., Civera, M., Lenticchia, E., Miraglia, G., Surace, C., & Ceravolo, R. (2022). Interferometric Satellite Data in Structural Health Monitoring: An Application to the Effects of the Construction of a Subway Line in the Urban Area of Rome. *Applied Sciences*, *12*(3), 1658. https://doi.org/10.3390/app12031658

Farneti, E., Cavalagli, N., Costantini, M., Trillo, F., Minati, F., Venanzi, I., & Ubertini, F. (2022). A method for structural monitoring of multispan bridges using satellite InSAR data with uncertainty quantification and its pre-collapse application to the Albiano-Magra Bridge in Italy. *Structural Health Monitoring*, 147592172210836. https://doi.org/10.1177/14759217221083609

Giordano, P. F., Iacovino, C., Quqa, S., & Limongelli, M. P. (2022). The value of seismic structural health monitoring for post-earthquake building evacuation. *Bulletin of Earthquake Engineering*. https://doi.org/10.1007/s10518-022-01375-2

Giordano, P., Turksezer, Z., Previtali, M., & Limongelli, M. (2022). Damage detection on a historic iron bridge using satellite DInSAR data. *Structural Health Monitoring*, 147592172110543. https://doi.org/10.1177/14759217211054350

ICOMOS/ISCARSAH. (2005). *Recommendations for the Analysis, Conservation and Structural Restoration of Architectural Heritage*.

Macchiarulo, V., Milillo, P., Blenkinsopp, C., & Giardina, G. (2022). Monitoring deformations of infrastructure networks: A fully automated GIS integration and analysis of InSAR time-series. *Structural Health Monitoring*, *21*(4), 1849–1878. https://doi.org/10.1177/14759217211045912

Miraglia, G., Lenticchia, E., Dabdoub, M., & Ceravolo, R. (2023). Satellite Interferometric Data and Perturbation Characteristics for Civil Structures at Nanohertz. *European Workshop on Structural Health Monitoring*, 604–612.

Rainieri, C., Notarangelo, M. A., & Fabbrocino, G. (2020). Experiences of Dynamic Identification and Monitoring of Bridges in Serviceability Conditions and after Hazardous Events. *Infrastructures*, *5*(10), 86. https://doi.org/10.3390/infrastructures5100086

Regione Lazio. (2020). *Open Data*. http://dati.lazio.it/catalog/it/dataset/serie-storica-agrometeo

repubblica.it. (2016). *Terremoto, danni ai tesori di Roma: crepe riaperte su San Paolo e su cupola Borromini a Sant’Ivo alla Sapienza*. https://roma.repubblica.it/cronaca/2016/10/30/news/terremoto_norcia_roma_basilica_di_san_paolo_basilica_san_lorenzo_scossa_7_40-150910836/

West, B. M., Locke, W. R., Andrews, T. C., Scheinker, A., & Farrar, C. R. (2019). Applying concepts of complexity to structural health monitoring. *Conference Proceedings of the Society for Experimental Mechanics Series*, *6*, 205–215. https://doi.org/10.1007/978-3-319-74476-6_27

Zhang, H., Reuland, Y., Chatzi, E., & Shan, J. (2023). *Near-Real Time Evaluation Method of Seismic Damage Based on Structural Health Monitoring Data* (pp. 114–122). https://doi.org/10.1007/978-3-031-07258-1_13